

Genome-Scale Metabolic Modeling Identifies Synergistic Metabolites that Enhance 5-Fluorouracil Efficacy in Colon Cancer

Hasan Rahimi-Tamandegani¹, Sayed-Amir Marashi², Ghazaleh Ghavami¹, Mahya Mehrmohamadi^{2*}, Soroush Sardari^{1*}

¹Drug Design and Bioinformatics Unit, Medical Biotechnology Department, Biotechnology Research Center, Pasteur Institute of Iran, Tehran, Iran; ²Department of Biotechnology, College of Science, University of Tehran, Tehran, Iran

OPEN ACCESS

Article type: Research Article

Received: July 19, 2025

Revised: August 19, 2025

Accepted: August 25, 2025

Published online: August 27, 2025

How to cite:

Rahimi-Tamandegani H, Marashi SA, Ghavami G, Mehrmohamadi M, Sardari S. Genome-Scale Metabolic Modeling Identifies Synergistic Metabolites that Enhance 5-Fluorouracil Efficacy in Colon Cancer. *Iran. Biomed. J.* 2025; 29(5): 321-334.



This article is licensed under a Creative Commons Attribution-NonDerivatives 4.0 International License.

ABSTRACT

Background: Colon cancer remains a leading cause of cancer-related mortality, with the efficacy of standard chemotherapy agents such as 5-FU limited by resistance and toxicity. This study aimed to identify metabolites that enhance 5-FU efficacy in CRC using GEM.

Methods: GEM was applied using the FVSEOF algorithm to identify metabolites that enhance the therapeutic efficacy of 5-FU in CRC. Context-specific metabolic models were constructed from TCGA data using the ftINIT algorithm. By simulating TS inhibition, we identified aspartate, lysine, and valine as candidate metabolites with altered uptake under constrained biomass production. Among them, lysine and valine are essential amino acids and were chosen for experimental validation using MTT assays and flow cytometry in HT-29 CRC cells and HU02 normal fibroblasts.

Results: Our approach identified aspartate, lysine, and valine as candidate synergistic metabolites. Experimental validation confirmed the strong synergy of lysine and valine with 5-FU in HT-29 cells, while showing significantly reduced effects in normal fibroblasts. Mechanistic analysis suggested that these amino acids enhance nucleotide demand and metabolic activity, amplifying 5-FU-induced stress.

Conclusion: This study demonstrates synergistic interventions and introduces amino acid co-supplementation as a potential strategy to improve CRC therapy with reduced toxicity. To our knowledge, this is the first study to employ GEM for the systematic prediction of metabolites that synergize with 5-FU, aiming to improve therapeutic outcomes in CRC.

DOI: 10.61882/ibj.5178

Keywords: Colorectal neoplasms, Computational biology, Drug synergism, Fluorouracil, Metabolic Networks and Pathways

Corresponding Authors:

Mahya Mehrmohammadi

Department of Biotechnology, College of Science, University of Tehran, Tehran, Iran; Tel.: (+98-21) 61112720; E-mail: mehrmohamadi@ut.ac.ir; ORCID ID: 0000-0002-6681-0810

Soroush Sardari

Drug Design and Bioinformatics Unit, Medical Biotechnology Department, Biotechnology Research Center, Pasteur Institute of Iran, Tehran, Iran; Tel.: (+98-21) 66954324; Fax: (+98-21) 66954324; E-mail: ssardari@hotmail.com; sardari@pasteur.ac.ir; ORCID ID: 0000-0003-2080-7402

List of Abbreviations:

5-FU: 5-fluorouracil; **CI:** combination Index; **CRC:** colon cancer; **DMEM:** Dulbecco's Modified Eagle Medium; **ELISA:** Enzyme-Linked Immunosorbent Assay; **FITC:** fluorescein isothiocyanate; **FPKM:** Fragments Per Kilobase Million; **FVSEOF:** Flux Variability Scanning based on Enforced Objective Flux; **GEM:** Genome-Scale Metabolic Model; **HT-29:** Human Colorectal Adenocarcinoma Cell Line; **HU02:** Human fibroblast cell line HU02; **MTT:** 3-(4,5-Dimethylthiazol-2-yl)-2,5-diphenyltetrazolium bromide assay; **RNA-seq:** RNA sequencing; **TCGA:** The Cancer Genome Atlas; **TCGA-COAD:** TCGA Colon Adenocarcinoma dataset; **TPM:** Transcripts Per Million; **TS:** thymidylate synthase; **t-SNE:** t-distributed Stochastic Neighbor Embedding

INTRODUCTION

Colon cancer poses a significant global health burden, with over 1.9 million new cases and approximately 904,000 deaths estimated in 2022, making it the third most common cancer and the second leading cause of cancer-related mortality^[1]. In the United States, there were an estimated 153,020 new CRC cases and 52,550 deaths in 2023. Projections for 2025 indicate a slight increase, with approximately 154,270 new cases and 52,900 deaths expected. These statistics underscore the persistent burden of CRC despite advances in screening and treatment^[2,3]. Incidence rates vary widely, with higher rates in developed regions like Europe and Northern America, reflecting differences in screening, lifestyle, and healthcare access. Despite advances in treatment, the five-year survival rate for advanced-stage CRC remains low at around 12%, underscoring the need for improved therapeutic strategies^[4].

5-FU has been a cornerstone of CRC chemotherapy since the 1950s, valued for its ability to inhibit DNA synthesis by targeting TS^[5]. However, its efficacy as a monotherapy is limited, with response rates in advanced CRC as low as 4.5% in some trials^[6]. Challenges include rapid drug metabolism by enzymes such as dihydropyrimidine dehydrogenase, leading to resistance and significant toxicities like leukopenia, which impacts patient quality of life^[7,8]. These limitations highlight the need for combination therapies to enhance the effectiveness of 5-FU.

Combination therapies, particularly those achieving synergistic effects, have shown promise in overcoming the shortcomings of 5-FU. Synergism, where the combined effect of agents exceeds the sum of their individual contributions, can improve therapeutic outcomes while reducing required doses and associated side effects^[9]. Research has suggested that combining 5-FU with other chemotherapeutic agents or natural compounds can increase response rates and survival times. For instance, interferon- β improved median survival from 7.2 to 15.9 months in advanced CRC^[6]. However, identifying optimal combinations remains challenging due to variability in patient responses and tumor subtypes^[10]. This study aimed to address these challenges by exploring metabolites that synergize with 5-FU to improve treatment efficacy in CRC.

Systems biology provides a powerful framework for dissecting the complex metabolic networks of cancer cells, integrating diverse datasets to uncover therapeutic opportunities. By combining high-throughput omics data—such as genomics, transcriptomics, and metabolomics—systems biology enables a holistic understanding of tumor metabolism, which is critical for

identifying interventions that enhance drug efficacy^[11]. This approach is particularly suited to CRC, where metabolic reprogramming supports tumor growth and contributes to resistance to treatments such as 5-FU. GEMs are central to this effort, offering mathematical representations of all known metabolic reactions within a cell, including gene-protein-reaction-metabolite associations^[12]. GEMs, such as Recon2 and HMR2, can be contextualized with CRC-specific data, including gene expression from the Cancer Cell Line Encyclopedia, to simulate tumor behavior under various conditions^[13]. These models predict how metabolites interact with drugs like 5-FU, identifying candidates that disrupt cancer cell metabolism synergistically^[14]. GEMs also enable patient stratification by metabolic profile, supporting personalized drug response predictions. By simulating metabolic changes, GEMs can identify combinations that enhance 5-FU efficacy and reduce toxicity, offering a solution to resistance driven by metabolic adaptation. We applied these models to systematically discover metabolites that act synergistically with 5-FU, with the ultimate aim of improving CRC therapy^[15].

Metabolic interventions have shown significant potential in enhancing the efficacy of chemotherapy, as evidenced by studies demonstrating improved response rates and clinical outcomes. For instance, supplementation with fish oil, rich in omega-3 fatty acids, nearly doubled response rates to first-line chemotherapy in lung cancer patients without increasing toxicity, suggesting that specific metabolites can modulate tumor metabolism to augment drug effects^[16]. Similarly, methionine restriction has been shown to synergize with 5-FU in CRC models, markedly inhibiting tumor growth by altering nucleotide metabolism and redox states, highlighting the therapeutic value of targeted dietary manipulations^[17]. Early nutritional interventions in head and neck cancer patients undergoing chemoradiotherapy also reduced treatment interruptions and improved outcomes, underscoring the broader applicability of metabolic strategies^[18]. In line with these findings, studies in mouse models have reported that increased serine availability induces resistance to 5-FU. Conversely, taurine supplementation exerts synergistic antitumor effects, and glutamine administration mitigates treatment-related mucositis^[19-21]. Despite these promising findings, a critical knowledge gap persists in systematically identifying and predicting metabolic interventions that enhance chemotherapy, particularly for CRC. While studies such as those on methionine restriction demonstrate synergy with 5-FU, the exploration of other metabolites remains limited and often empirical^[22]. Current research lacks

comprehensive approaches that use systems biology tools, such as GEMs, to predict which metabolites can synergize with 5-FU across diverse CRC subtypes. Despite their capacity to integrate multi-omics data for reconstructing tumor-specific metabolic networks, GEMs have seen limited application in this area. This study aimed to address this gap by employing context-specific metabolic modeling to systematically identify novel metabolites that enhance 5-FU efficacy, paving the way for more effective and personalized treatment strategies.

To the best of our knowledge, this is the first study to use GEMs for the systematic identification of metabolites that synergize with 5-FU, and its findings may open new avenues for metabolically informed cancer therapies.

MATERIALS AND METHODS

Gene expression data acquisition

Gene expression (RNA-seq) and clinical data for colon adenocarcinoma (TCGA-COAD) primary tumor samples and normal samples were retrieved from TCGA using the TCGABiolinks package in R^[23]. These data were used to reconstruct CRC-specific metabolic networks. Additionally, gene expression data for normal samples of gastric, breast, and lung tissues were included to compare algorithms for generating context-specific metabolic models, ensuring robust model performance before application in CRC.

Model selection and comparison

To identify the optimal algorithm for constructing context-specific metabolic models of CRC, we generated models for normal samples from colon, gastric, breast, and lung tissues using three algorithms: GIMME (Gene Inactivity Moderated by Metabolism and Expression)^[24], INIT (Integrative Network Inference for Tissues)^[25], and ftINIT (fast task-driven Integrative Network Inference for Tissues)^[26]. GIMME was implemented in the COBRA Toolbox version 3.0^[27], while tINIT and ftINIT were run in RAVEN^[28], using the HUMAN-GEM model as the metabolic template. Multiple gene expression cut-off thresholds were tested to assess algorithm robustness. Model similarity within the same tissue type and differences across tissues were evaluated using the Jaccard index of reaction overlap. A binary reaction content matrix (indicating active reactions per model) was subjected to t-SNE dimension reduction and visualized as scatter plots to confirm tissue-specific clustering.

Context-specific model development

The ftINIT algorithm, chosen for its performance in prior comparisons (see Results), was used to construct context-specific metabolic models for CRC samples. Gene expression data in TPM from TCGA-COAD were mapped to reactions using the gene-protein-reaction rules from HUMAN-GEM model, with HUMAN-GEM as the reference metabolic model. IModels were generated for each tumor sample using the RAVEN Toolbox, with Gurobi as the optimization solver for efficient computation. To assess model quality, a binary reaction content matrix (indicating active reactions) was subjected to t-SNE dimension reduction and visualized as scatter plots to confirm cancer-specific metabolic profiles.

Model integration

To generate representative metabolic models for CRC and normal colon tissue, we extracted reactions active in at least 50% of individual models derived from colon cancer and normal colon samples (TCGA-COAD). This 50% threshold was selected based on sensitivity analyses to balance the inclusion of shared reactions with tissue specificity. Using ftINIT-generated models from HUMAN-GEM, reaction extraction and merging were performed in the RAVEN Toolbox. Core reactions, defined as those present in 50% or more of models, were combined into a union set while retaining the gene-protein-reaction rules of HUMAN-GEM. This process resulted in two models: one indicating CRC metabolism and the other representing normal colon metabolism.

Forced biomass reduction modeling

To further analyze the metabolic effects of 5-FU, the FVSEOF algorithm was applied to both the cancerous and normal metabolic models^[29]. We conducted this step to model how a forced reduction in biomass production in the presence of 5-FU influences the activity of other reactions within the metabolic network. The FVSEOF algorithm progressively reduced biomass flux while monitoring the corresponding changes in the flux of other reactions. The output consisted of a comprehensive list of metabolic reactions whose fluxes were altered during the forced reduction of biomass. These reactions were categorized based on whether their fluxes increased or decreased. Both types of flux changes were evaluated for their potential contribution to reduced biomass production, providing insights into how 5-FU affects metabolic pathways linked to cell growth and survival.

Simulation of amino acid uptake under metabolic stress

To model differential metabolic responses under therapeutic stress, flux balance analysis was performed on individual cancer and healthy tissue-specific metabolic models. Baseline flux distributions were calculated to determine the uptake fluxes of valine and lysine. An essential reaction targeted by 5-FU was then constrained to 20% of its baseline flux to simulate partial enzymatic inhibition. Under these constrained conditions, flux balance analysis was repeated, and amino acid uptake fluxes were evaluated. Samples were categorized based on whether their amino acid uptake fluxes remained above 20% of baseline (indicating preserved uptake capacity), approximated 20% (proportional reduction), or fell below 20% of baseline values.

Cell culture

The HT-29 human colorectal adenocarcinoma cell line (IBRC C10097, Iranian Biological Resource Center) was cultured in DMEM/F12 medium (Gibco, USA) supplemented with 10% fetal bovine serum, 100 µg/mL of streptomycin, 100 U/mL of penicillin, and 2 mM of L-glutamine. Cells were maintained in a humidified atmosphere with 95% humidity and 5% CO₂ at 37 °C to ensure optimal growth. These conditions supported cell proliferation and reproducibility for subsequent assays to validate computational predictions of 5-FU synergistic metabolites.

MTT assay

To evaluate the survival of HT-29 CRC cells, the MTT assay was performed using metabolites predicted by FVSEOF analysis with 5-FU. Solid compounds were dissolved in 1 ml of DMSO or phosphate-buffered saline, depending on solubility, to create stock solutions exceeding the highest tested concentration. Serial dilutions were then prepared in DMEM/F12 medium to obtain six concentrations (0.1–100 µM). For the assay, 100 µl of DMEM/F12 medium supplemented with 10% fetal bovine serum containing 12,000 cells was added to each well of a 96-well plate. Plates were incubated with 5% CO₂ at 37 °C for 24 hours to allow cell adherence. The medium was then removed, and wells were treated with compound dilutions, 5-FU (positive control) or solvent vehicle (negative control) for 48 hours. After treatment, 20 µl of MTT dye (5 mg/ml in phosphate-buffered saline) was added per well, and plates were incubated for 3–4 hours. The medium and MTT dye were removed, and 100 µl of DMSO was added to dissolve formazan crystals. After 15 minutes, absorbance was measured at 545 nm (with 630 nm as background) using an ELISA reader to assess cell viability. MTT results were subsequently analyzed

using Compusyn software version 1.0 to evaluate potential synergistic effects between 5-FU and the tested metabolites^[30].

Flow cytometry

To investigate the cell death mechanisms induced by metabolites synergistic with 5-FU, flow cytometry was performed using Annexin V/PI staining on HT-29 CRC cells (see Cell Culture). Cells were cultured in T25 flasks with DMEM/F12 medium until ~80% confluence. After removing the medium, cells were treated under three conditions: (1) 5-FU alone at its IC₅₀ concentration (determined by MTT assay), (2) 5-FU at 1/5 × IC₅₀ combined with each FVSEOF-predicted metabolite at 100 µg/ml, or (3) an untreated control. Cells were incubated in a humidified incubator with 5% CO₂ at 37 °C for 48 hours, then trypsinized, harvested, and stained with Annexin V-FITC and propidium iodide using a commercial kit (BD Biosciences, New Jersey). Flow cytometry analysis distinguished viable, early apoptotic, late apoptotic, and necrotic cells.

RESULTS

Algorithm selection and model construction

As illustrated in the schematic overview of the computational workflow presented in Figure 1A, gene expression datasets were retrieved and analyzed to construct accurate context-specific GEMs for normal tissues. RNA-seq expression data from 25 normal samples, each from colon, gastric, lung, and breast tissues, were obtained from TCGA using the TCGA biolinks package in R, in both TPM and FPKM formats. These datasets provided the foundation for building and evaluating tissue-specific metabolic models. To identify the optimal algorithm for context-specific model construction, we compared three reconstruction methods—GIMME, INIT, and ftINIT—and applied them to the collected expression data. GIMME was implemented using FPKM data with two thresholding strategies: a fixed threshold of 2.5 and a modified thresholding scheme based on a minimum (1.2 FPKM) and maximum (5 FPKM) range. In this modified version, genes below the minimum threshold were considered inactive, those above the maximum were active, and genes within the range were evaluated based on their mean FPKM across all tissues. For INIT and ftINIT, TPM expression data were used. Three thresholding approaches were tested for ftINIT: (1) a fixed threshold of 1 TPM, (2) the mean TPM across all samples, and (3) the mean TPM per tissue type (i.e., tissue-specific mean thresholding). All models were constructed using the HUMAN-GEM metabolic template, and the resulting reaction content was

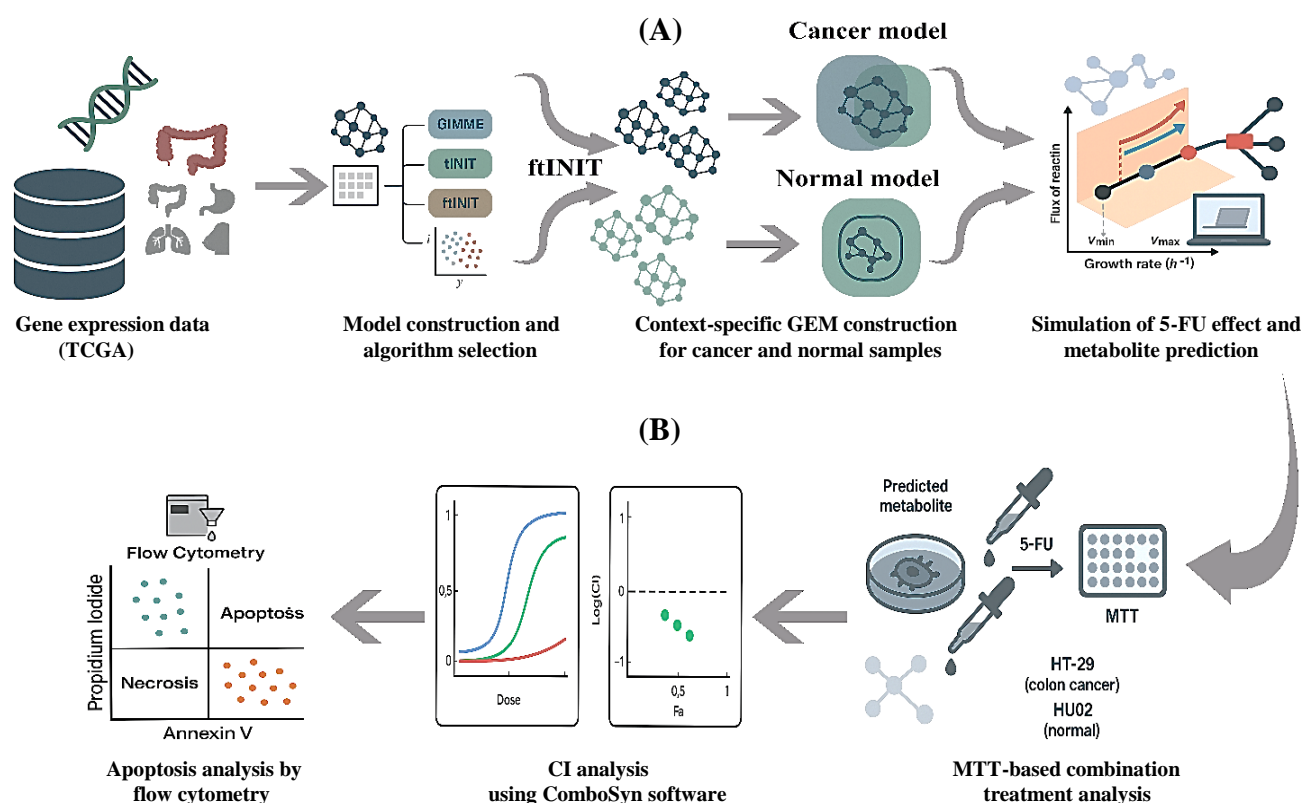


Fig. 1. Integrated computational and experimental workflow for identifying 5-FU synergistic metabolites. (A) Computational pipeline for constructing context-specific metabolic models and identifying synergistic metabolites using FVSEOF. (B) Experimental workflow illustrating cell culture, MTT assay, and flow cytometry procedures for validating predicted metabolite-5-FU synergies.

encoded as binary matrices to represent the presence or absence of reactions per model. To assess the ability of the algorithms to generate biologically relevant, tissue-specific models, we applied t-SNE to the binary reaction matrices to visualize clustering by tissue type (Fig. 2). A detailed comparison of algorithms and thresholding strategies is summarized in Supplementary Table S1, highlighting the different performance outcomes. The results revealed that modified thresholding improved the ability of GIMME to distinguish between tissues and ftINIT, particularly when using tissue-specific mean thresholds, which produced the most distinct and consistent clustering of models by tissue type. Given its ability to generate the most distinct and consistent clustering of tissue-specific models, ftINIT with tissue-specific mean thresholds was chosen as the optimal algorithm, thereby ensuring biological relevance for subsequent CRC GEM reconstruction.

Context-specific GEM integration

Following algorithm selection, RNA-seq data for CRC tissue samples from patients who had received adjuvant 5-FU therapy were obtained from TCGA-COAD using the TCGAbiLinks package in R (Fig. 3A).

TPM-formatted gene expression data were used to construct metabolic models for both CRC and normal colon tissue samples using the ftINIT algorithm, the HUMAN-GEM reference model, and TPM gene expression data. Model reconstruction was performed in the RAVEN Toolbox with Gurobi as the optimization solver. For thresholding, mean TPM expression values were applied—cancer-specific means for tumor samples and colon-specific means for normal samples. Tumor and normal metabolic models differed in both the average number of reactions and the sets of unique reactions present in each group, reflecting distinct underlying metabolic architecture (Fig. 3B). To assess whether these models could effectively differentiate between tumor and normal metabolic states, reaction content was represented as binary presence/absence matrices. A t-SNE dimensionality reduction was then applied to these matrices. The resulting two-dimensional scatter plot (Fig. 3C) demonstrated a clear separation between cancerous and normal samples, confirming that the models successfully captured distinct metabolic features associated with each tissue type. To further facilitate comparative analysis and simulation, we constructed

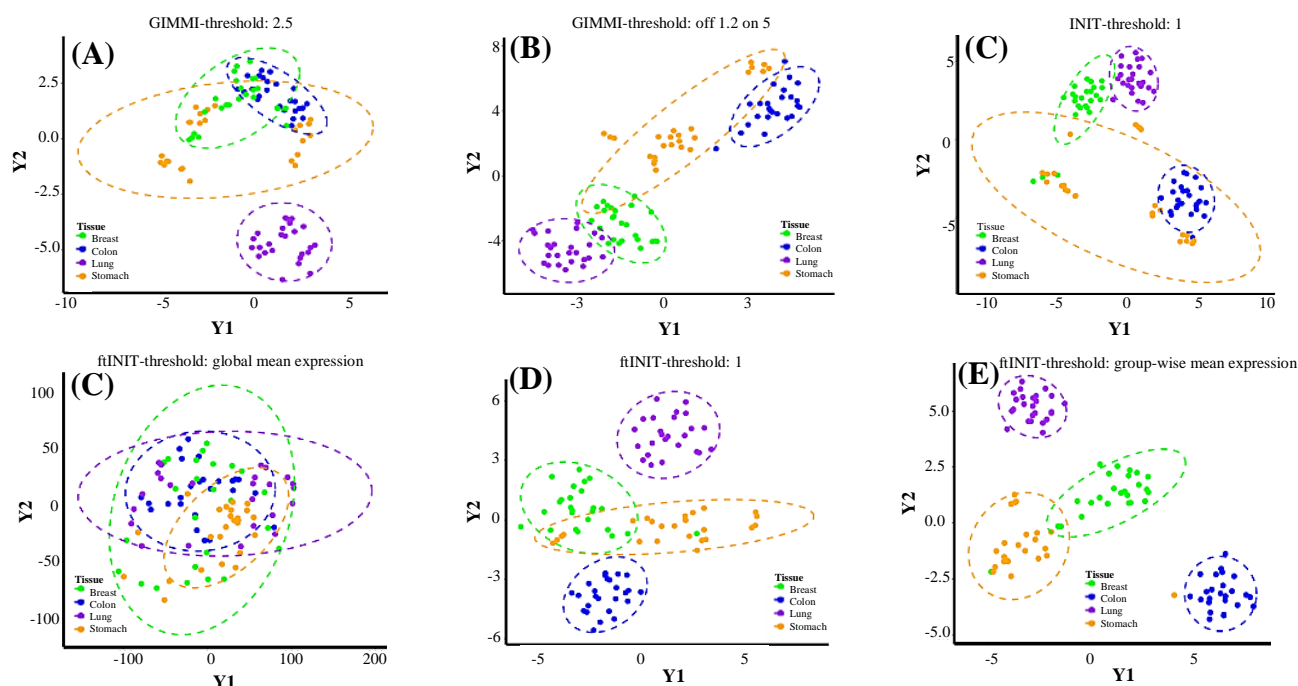


Fig. 2. t-SNE plots comparing tissue-specific separation across different algorithms and thresholding strategies for metabolic model construction. (A) GIMME with a fixed threshold of 2.5 shows partial tissue clustering; (B) GIMME with off/on thresholding (1.2/5) improves tissue separation, notably distinguishing lung and colon; (C) INIT with a threshold of 1 provides limited separation among tissue types; (D) ftINIT with a global mean expression threshold results in overlapping clusters, suggesting low tissue specificity; (E) ftINIT with a fixed threshold of 1 enhances separation compared to tINIT; (F) ftINIT with a group-wise mean expression threshold yields the clearest tissue-specific clusters, particularly for colon and breast tissues, and was selected for further modeling.

integrated metabolic models for both cancerous and normal colon tissues. Integration was achieved by merging reactions present in at least 50% of the individual models within each group. This 50% threshold, based on the previously generated ftINIT models, balanced tissue specificity with reaction coverage. The integration process, conducted in the RAVEN Toolbox, resulted in two representative models: one capturing the core metabolic features of CRC and the other representing normal colon tissue metabolism. These context-specific consensus models provided a robust foundation for subsequent flux-based analyses, including simulation of 5-FU action and prediction of synergistic metabolite interventions tailored to the metabolic landscape of CRC.

Simulation of 5-FU effect and metabolite prediction

To identify metabolic interventions that could enhance the therapeutic efficacy of 5-FU, we applied the FVSEOF algorithm to the integrated cancer-specific and normal colon tissue models. This simulation was performed in the COBRA Toolbox to detect reactions whose feasible flux ranges were altered in response to reduced biomass production, mimicking the inhibitory action of 5-FU. Specifically, the FVSEOF algorithm simulated the progressive suppression of biomass flux by constraining the activity of TS, the primary target of

5-FU. The resulting flux distributions revealed reactions whose minimum or maximum feasible flux values shifted under this constraint. Among these reactions, metabolite uptake reactions exhibiting altered flux ranges were prioritized as potential synergistic candidates with 5-FU. In the CRC model, the uptake flux ranges of lysine, valine, and aspartate were affected by enforced biomass reduction. In the normal colon model, lysine and aspartate uptake ranges were also affected, whereas the phosphatidylethanolamine flux range was uniquely influenced. These results indicate that metabolite uptake ranges are differentially modulated in tumor metabolism under 5-FU stress, potentially amplifying the cytotoxic effects of the drug. Among the identified candidates, valine and lysine, as essential amino acids, were chosen for further analysis.

Metabolic vulnerabilities revealed by amino acid uptake under drug stress

To further investigate metabolic involvement in therapeutic response, we simulated partial blockade of the TS reaction (the primary target of 5-FU) by constraining its flux to 20% of baseline values across individual cancer and normal tissue-specific models. To this end, flux balance analysis was first conducted for each model under normal (drug-free) conditions to obtain baseline fluxes, including the TS flux (V_{ts}) and

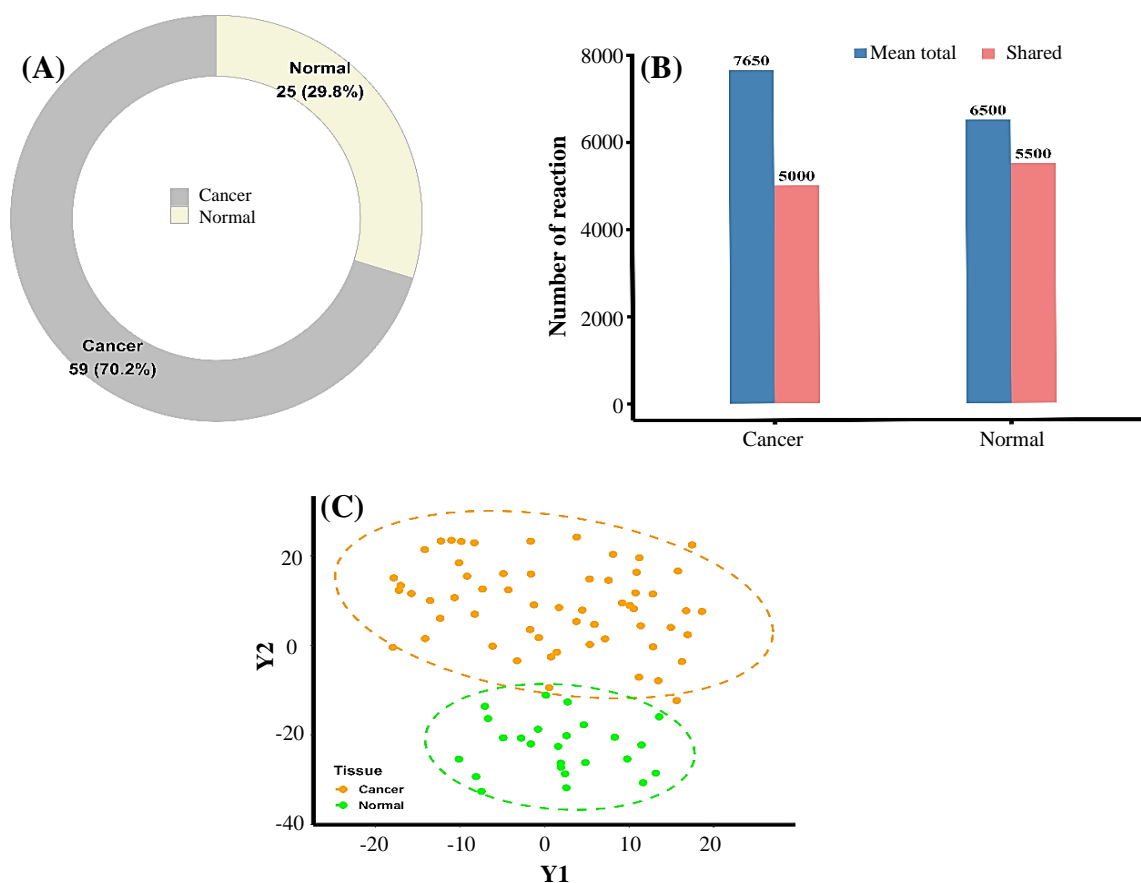


Fig. 3. Comparative analysis of CRC and normal metabolic models. (A) Sample distribution of the TCGA-COAD dataset, showing the number of CRC and normal samples used for model generation; (B) Comparison of the average number of reactions and shared reactions between cancer-specific and normal metabolic models, highlighting distinct metabolic architectures; (C) t-SNE plot demonstrating the separation between cancer and normal colon metabolic models based on reaction content.

the uptake fluxes of valine (V_{val}) and lysine (V_{lys}). Subsequently, the TS flux was restricted to 0.2× valine to simulate partial drug inhibition, expected to reduce biomass production. Uptake fluxes were then evaluated relative to the 20% TS constraint, without requiring proportional scaling. Under these stress conditions, we then analyzed the uptake fluxes of valine and lysine under these stress conditions. Notably, normal tissue models more frequently maintained elevated amino acid uptake compared to cancer sample models. Specifically, 28.0% of normal sample models versus 21.8% of cancer sample models sustained valine uptake above the expected proportional reduction. Similarly, 40.0% of normal sample models versus 30.5% of cancer sample models maintained elevated lysine uptake (Fig. 4). These findings suggest that, compared to CRC cell lines, normal epithelial cells retain a superior capacity to consume excess valine and lysine under 5-FU-induced metabolic stress. This difference likely reflects variations in metabolic flexibility and mitochondrial

function. Previous studies have shown that 5-FU alters the expression of genes involved in amino acid metabolism and oxidative phosphorylation in CRC cells^[31,32]. In contrast, normal cells maintain more robust mitochondrial oxidation and redox control, enabling efficient catabolism of these amino acids and reducing the accumulation of toxic intermediates^[33]. This difference in uptake has important therapeutic implications, as both amino acids generate highly toxic intermediates during catabolism. Valine metabolism produces methacrylyl-CoA and methylmalonyl-CoA^[34,35], while lysine catabolism generates saccharopine, α-amino adipic semialdehyde, and piperidine-6-carboxylate^[36,37], all of which are documented cytotoxic compounds. The higher consumption rates observed in normal cells suggest a greater tolerance for these compounds, while the relatively lower uptake in cancer cells may lead to enhanced cytotoxicity when valine and lysine are supplemented in combination with 5-FU.

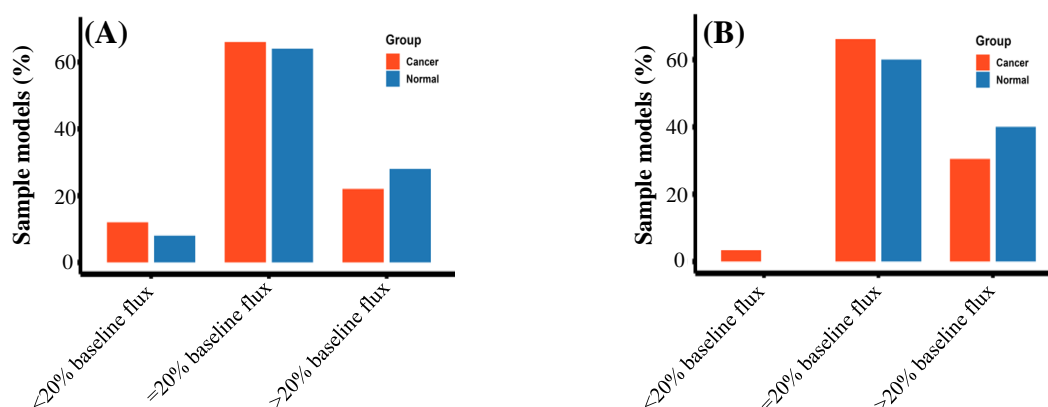


Fig. 4. Distribution of sample models by (A) valine and (B) lysine uptake response to simulated drug inhibition. For each sample model (cancer and normal), the uptake flux of the indicated amino acid was examined after constraining an essential reaction to 20% of its baseline value (to mimic drug-induced inhibition). Sample models were categorized based on whether their amino acid uptake fluxes decreased to a level greater than, similar to, or lower than the expected proportional baseline (20% of the original uptake).

Combination effect of 5-FU with predicted metabolites in cancer and normal cells

As outlined in the experimental workflow (Fig. 1A), cytotoxicity assays were conducted to experimentally validate the synergistic potential of valine and lysine. These assays were performed using HT-29, as a CRC cell line, and HU02, as a normal fibroblast cell line. Initial evaluations focused on determining the toxicity profiles of 5-FU and two candidate metabolites—lysine and valine—administered as single agents individually. Cells were treated with a wide range of concentrations (10,000, 2,000, 400, 80, 16, and 3.2 $\mu\text{g/ml}$ for metabolites and 400, 80, 16, 3.2, 25, 12.5, 6.25, 3.12, 0.64, and 0.128 $\mu\text{g/ml}$ for 5-FU), allowing for the generation of dose-response curves and calculation of IC_{50} values, which provided a foundation for assessing therapeutic index and selectivity. Based on the IC_{50} data (Table 1), combination treatments were then designed to explore potential synergistic interactions between 5-FU and selected metabolites. Lysine, valine, and phenylalanine (used as a negative control) were combined with 5-FU at concentrations corresponding to IC_{50} , $1/5 \times \text{IC}_{50}$, and $1/10 \times \text{IC}_{50}$, and tested in both HT-29 and HU02 cells using the MTT assay. Viability data were analyzed using the CI method via Compusyn

software to assess the nature of drug interactions. In HT-29 cancer cells, combinations of 5-FU with lysine and valine exhibited synergistic effects across all tested concentrations, as indicated by CI values less than one. In contrast, phenylalanine showed no synergistic effect, confirming its role as a negative control (Table 2 and Fig. S1A-S1C). To further illustrate these differences, we generated the corresponding dose-response curves for each treatment, which clearly displayed the IC_{50} shifts and the concentration-dependent reduction in cell viability (Fig. S2A-S2C). Notably, when these combinations were tested in HU02 normal fibroblast cells, their effects were distinctly attenuated (Table 3 and Fig. S1D-S1F). These metabolites exhibited weak synergistic effects with 5-FU at higher concentrations ($\geq \text{IC}_{50}$), whereas at a lower concentration ($1/10 \times \text{IC}_{50}$), unlike in HT-29 cancer cells that displayed strong synergy, they showed no synergistic effect. Consistent with these results, the corresponding dose-response curves confirmed the attenuated response in normal cells (Fig. S2D-S2F). These differential responses highlight cancer cell selectivity, suggesting that lysine and valine—particularly in combination with 5-FU—may enhance therapeutic outcomes in CRC while limiting toxicity to normal tissue.

Table 1. IC_{50} values of candidate compounds on the HT-29 CRC cell and HU02 normal cell line

| Sample | IC_{50} (μM) on HT-29 cell line | IC_{50} (μM) on HU02 cell line |
|---------------|---|--|
| Lysine | >68,400 | >68,400 |
| Valine | >85,400 | >85,400 |
| Phenylalanine | >60,600 | > 60,600 |
| Fluorouracil | 101.0 ± 0.09 | 44.1 ± 0.07 |

Data are presented as the mean \pm standard deviation (SD) of three independent replicates ($n = 3$), with 95% confidence intervals.

Table 2. CI values and cell viability percentage for 5-FU combined with selected metabolites at various concentrations in the HT-29 cell line

| 5-FU ($\mu\text{g/ml}^*$) | Metabolite ($\mu\text{g/ml}^*$) | Effect% (Lys) [**p value] | CI (Lys) | Effect% (Val) [**p value] | CI (Val) | Effect% (Phe) [**p value] | CI (Phe) |
|--------------------------------|--------------------------------------|---------------------------------------|-------------|---------------------------------------|-------------|---------------------------------------|-------------|
| 20.0 | 1000.0 | 0.599 [0.9] | 0.81431 | 0.622 [0.35] | 0.93916 | 0.430 [0.008] | 2.98287 |
| 20.0 | 100.0 | 0.571 [0.9] | 0.78617 | 0.591 [0.43] | 0.75974 | 0.379 [0.001] | 3.16612 |
| 20.0 | 10.0 | 0.454 [0.6] | 0.85269 | 0.537 [0.65] | 0.87897 | 0.363 [0.002] | 3.42664 |
| 4.0 | 1000.0 | 0.484 [7e-05] | 0.27688 | 0.541 [3e-05] | 0.51275 | 0.39 [0.03] | 1.37726 |
| 4.0 | 100.0 | 0.482 [0.0001] | 0.21766 | 0.539 [3e-05] | 0.20808 | 0.31 [0.003] | 1.07213 |
| 4.0 | 10.0 | 0.439 [0.01] | 0.24363 | 0.454 [0.001] | 0.23505 | 0.274 [0.03] | 1.27879 |
| 2.0 | 1000.0 | 0.450 [0.0001] | 0.19927 | 0.527 [5e-05] | 0.44083 | 0.04 [1e-05] | 20.4012 |
| 2.0 | 100.0 | 0.440 [0.001] | 0.12856 | 0.485 [4e-04] | 0.14243 | 0.02 [3e-05] | 50.8750 |
| 2.0 | 10.0 | 0.419 [0.02] | 0.13055 | 0.451 [9e-05] | 0.12077 | 7.0E-4 [4e-04] | 7930.04 |

*At the tested concentrations, approximate molar equivalents are: 5-FU (20, 4, 2 $\mu\text{g/ml} \approx 154, 31, 15 \mu\text{M}$), lysine (1000, 100, 10 $\mu\text{g/ml} \approx 6840, 684, 68 \mu\text{M}$), valine (1000, 100, 10 $\mu\text{g/ml} \approx 8536, 854, 85 \mu\text{M}$), and phenylalanine (1000, 100, 10 $\mu\text{g/ml} \approx 6054, 605, 61 \mu\text{M}$);

**In comparison to 5-FU alone

Flow-cytometric assessment of apoptosis induced by 5-FU and its metabolite combinations

Flow cytometric analysis using Annexin V-FITC/PI staining was performed to investigate the mechanism of cell death induced by 5-FU and its combination with FVSEOF-identified metabolites in the HT-29 CRC cell line (Fig. 5). In the untreated control group, 73.5% of cells remained viable, with 23.1% undergoing apoptosis and 3.33% indicating necrosis. Treatment with 5-FU at its IC_{50} concentration increased cell death, resulting in 36.4% apoptotic and 22.5% necrotic cells, reducing viable cells to 41.1%. Notably, when 5-FU was administered at $1/5 \times \text{IC}_{50}$ in combination with lysine or valine (100 $\mu\text{g/ml}$), apoptosis was significantly enhanced with minimal necrosis. Specifically, valine induced 51.2% apoptosis with 0.94% necrosis, while lysine induced 53.8% apoptosis with 1.49% necrosis. These findings demonstrate that even at the reduced 5-FU concentrations, co-treatment with lysine or valine enhances apoptotic cell death while minimizing necrotic damage, which suggests

a targeted and less toxic mechanism for effective CRC therapies.

DISCUSSION

This study introduces a novel application of the FVSEOF algorithm to identify metabolites that synergize with 5-FU treatment in CRC. In vitro validation demonstrated that FVSEOF-predicted metabolites, lysine and valine, exhibited synergy with 5-FU in HT-29 CRC cells, as confirmed by CI analysis. Although phenylalanine, included as a negative control, did not show synergy, it displayed an interesting antagonistic behavior that needs investigation in future studies. These combinations were selective for cancer cells compared to normal HU02 fibroblasts, suggesting targeted therapeutic potential. Flow cytometry analysis confirmed that these combinations significantly enhanced apoptosis while minimizing necrosis, even at the reduced 5-FU concentrations.

Table 3. CI values and cell viability effects for 5-FU combined with selected metabolites at various concentrations in HU02 cell line

| 5-FU ($\mu\text{g/ml}^*$) | Metabolite ($\mu\text{g/ml}^*$) | Effect% (Lys) [$**p$ value] | CI (Lys) | Effect% (Val) [$**p$ value] | CI (Val) | Effect% (Phe) [$**p$ value] | CI (Phe) |
|--------------------------------|--------------------------------------|---------------------------------|-------------|---------------------------------|-------------|---------------------------------|-------------|
| 20.0 | 1000.0 | 0.705 [8e-05] | 0.66143 | 0.691 [.0001] | 0.67071 | 0.557 [0.003] | 2.48045 |
| 20.0 | 100.0 | 0.702 [2e-04] | 0.58704 | 0.677 [0.003] | 0.74033 | 0.512 [0.0001] | 3.2015 |
| 20.0 | 10.0 | 0.691 [2e-04] | 0.64458 | 0.668 [0.008] | 0.80402 | 0.503 [0.002] | 3.3909 |
| 4.0 | 1000.0 | 0.673 [0.005] | 0.26291 | 0.627 [0.01] | 0.26694 | 0.466 [0.0001] | 1.3156 |
| 4.0 | 100.0 | 0.583 [0.02] | 0.35906 | 0.595 [0.009] | 0.31504 | 0.399 [1e-05] | 1.7025 |
| 4.0 | 10.0 | 0.469 [0.03] | 0.91050 | 0.495 [0.1] | 0.73042 | 0.384 [8e-04] | 1.8923 |
| 2.0 | 1000.0 | 0.383 [0.3] | 1.15269 | 0.214 [0.2] | 5.50250 | 0.386 [0.09] | 1.38063 |
| 2.0 | 100.0 | 0.35 [0.9] | 1.30856 | 0.125 [0.001] | 21.0121 | 0.324 [0.7] | 1.6827 |
| 2.0 | 10.0 | 0.201 [0.1] | 6.38713 | 0.037 [0.01] | 332.817 | 0.321 [0.6] | 1.6984 |

*At the tested concentrations, approximate molar equivalents are: 5-FU (20, 4, 2 $\mu\text{g/ml} \approx 154, 31, 15 \mu\text{M}$), lysine (1000, 100, 10 $\mu\text{g/ml} \approx 6840, 684, 68 \mu\text{M}$), valine (1000, 100, 10 $\mu\text{g/ml} \approx 8536, 854, 85 \mu\text{M}$), and phenylalanine (1000, 100, 10 $\mu\text{g/ml} \approx 6054, 605, 61 \mu\text{M}$);

**in comparison to 5-FU alone

The synergistic interactions observed between 5-FU and the selected amino acids, particularly lysine and valine, can be mechanistically interpreted through their metabolic contributions in cancer cell metabolism. Lysine is catabolized into acetyl-CoA, a TCA cycle intermediate, potentially contributing to biosynthetic and energy-generating pathways under certain metabolic conditions^[38]. This metabolic activation may increase the demand for deoxynucleotides. By inhibiting TS, 5-FU disrupts their synthesis, thereby inducing replication stress and enhancing cytotoxicity. Valine follows a similar rationale, as it is catabolized into succinyl-CoA, contributing to the TCA cycle and modestly supporting anabolic activity, particularly when other energy sources are limited^[39]. Such metabolic activation could potentially amplify the cytotoxic effects of 5-FU by increasing the sensitivity of proliferating cells to dTMP depletion. While these interpretations align with known metabolic functions of the amino acids, it is important to note that our

predictions stem from a constraint-based metabolic modeling framework that does not capture regulatory or signaling dynamics. For example, lysine may influence histone acetylation and epigenetic states, while valine may modulate mTOR signaling, mechanisms that fall outside the scope of GEMs^[40,41]. Both histone acetylation and mTOR signaling are closely linked to apoptotic regulation, suggesting that the observed enhancement of 5-FU-induced apoptosis may, at least in part, be mediated through these pathways. Considering these constraints and the emergent nature of the predicted synergies, additional studies—such as metabolomics, fluxomics, and pathway-specific analyses—are needed to fully elucidate the underlying biological mechanisms.

Metabolic modeling has transformed our understanding of cancer cell vulnerabilities, but its application to chemotherapy enhancement remains limited^[12]. The FVSEO algorithm was initially developed to identify gene or reaction targets that

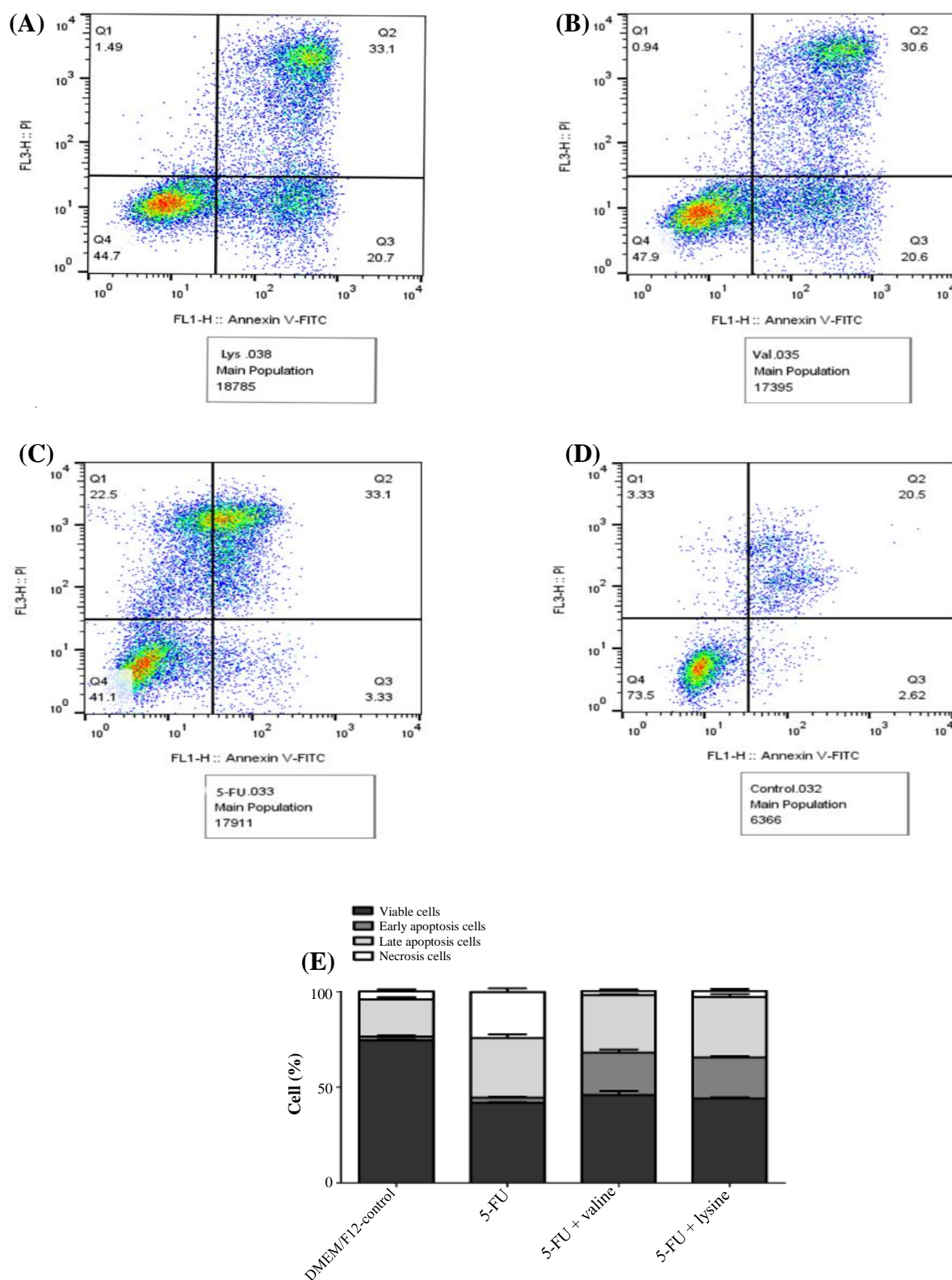


Fig. 5. Flow cytometry analysis (annexin V/PI staining) of HT-29 CRC cells treated with 5-FU and its synergistic metabolites. Cells were stained with annexin V-FITC and propidium iodide to assess early apoptosis (Q3), late apoptosis (Q2), necrosis (Q1), and viable cells (Q4). (A) 5-FU + lysine: enhancement of late (33.1%) and early (20.7%) apoptosis; (B) 5-FU + valine: similar profile with late (30.6%) and early (20.6%) apoptosis; (C) 5-FU alone: late (33.1%) and early (3.3%) apoptosis, indicating necrotic shift; (D) DMEM/F12 as negative control; (E) cytotoxic effect of 5-FU alone and in combination with valine or lysine on HT-29 cell line. Data are presented as the mean \pm SD of three independent replicates ($n = 3$), with 95% CIs.

enhance metabolite production in bioprocess optimization. It has since been successfully adapted for culture medium optimization across both mammalian and microbial systems^[29,42,43]. However, to our knowledge, this is the first study applying FVSEOF to predict synergistic metabolites for chemotherapy enhancement in cancer cells. By simulating TS inhibition, FVSEOF successfully identified metabolites whose metabolic uptake fluxes were altered under constrained biomass production, pinpointing aspartate, lysine, and valine as candidates.

In our study, additional computational modeling using flux balance analysis revealed a critical metabolic distinction. Normal colon sample models demonstrated superior capacity to maintain amino acid uptake under simulated drug stress compared to cancer cell models. This differential uptake pattern provides a mechanistic explanation for the selective enhancement of 5-FU efficacy observed experimentally. The therapeutic implications may arise from the toxic nature of lysine and valine metabolic intermediates. Lysine catabolism generates highly cytotoxic compounds, including saccharopine, α -amino adipic semialdehyde, and piperidine-6-carboxylate, while valine metabolism produces methacrylyl-CoA and methylmalonyl-CoA, both established as toxic intermediates. When excess lysine and valine are supplemented, these toxic metabolites accumulate within cells. However, the superior uptake capacity of healthy cells suggests that they can more rapidly consume the supplemented amino acids and manage toxic intermediates. In contrast, the lower uptake capacity of cancer cells suggests that accumulation of these cytotoxic metabolites makes cancer cells more vulnerable to the combined treatment. This mechanism explains the selective cytotoxicity observed in our experimental validation and corroborates the potential for amino acid co-supplementation as a strategy to improve the therapeutic effectiveness of 5-FU. The computational predictions, combined with the known toxicity of metabolic intermediates, provide a rational basis for this metabolic vulnerability-based approach to cancer therapy.

Previous studies have demonstrated that metabolic interventions, such as omega-3 fatty acid or taurine supplementation and methionine restriction, can sensitize tumors to chemotherapy by modulating metabolic pathways^[17,21,22,44]. Our findings align with these observations, extend the concept by identifying specific metabolites—lysine and valine—as novel modulators of 5-FU efficacy. Unlike earlier empirical approaches, our study employs systems biology-driven prediction, offering a targeted and mechanistically informed strategy for metabolic intervention.

The discovery that lysine and valine can synergize with 5-FU opens new avenues for CRC therapy.

Supplementation with these amino acids could allow for lower effective doses of 5-FU, potentially reducing systemic toxicity while maintaining or even enhancing therapeutic outcomes. Given their dietary origin and biocompatibility, these metabolites represent promising, accessible adjuncts to standard chemotherapy regimens. Despite these promising results, the findings of this study are limited to *in vitro* assays using a single CRC cell line (HT-29) and a normal fibroblastic cell line (HU02). Broader validation across multiple cell lines and *in vivo* models is necessary. Additionally, while metabolic mechanisms have been proposed, detailed metabolomic analyses are needed to further elucidate the exact pathways contributing to the observed synergy. Clinical trials evaluating 5-FU in combination with lysine and valine supplementation could substantiate the translational potential of these findings. Furthermore, refining FVSEOF by integrating multi-omics datasets could enhance its predictive accuracy for broader applications in cancer therapy.

CONCLUSION

This study establishes FVSEOF as an effective and versatile tool for predicting synergistic metabolic interventions in cancer therapy. By integrating GEM with experimental validation, we identified specific amino acids—lysine and valine—that can selectively enhance the cytotoxicity of 5-FU in CRC cells. These findings highlight the potential of metabolically informed strategies to improve the efficacy and specificity of chemotherapy. The proposed approach offers a promising direction for developing adjunct therapies that exploit tumor metabolism while minimizing toxicity to normal tissues.

DECLARATIONS

Acknowledgments

We acknowledge the use of ChatGPT (OpenAI) for language editing-grammar and spell check to improve the clarity and flow of the manuscript. All scientific content, data interpretation, and conclusions remain entirely the responsibility of the authors.

Ethical approval

All the procedures in this study were approved by the Ethics Committee of Pasteur Institute of Iran, Tehran (ethical code: IR.PIL.REC.1403.011).

Consent to participate

Not applicable.

Consent for publication

All authors reviewed the results and approved the final version of the manuscript.

Authors' contributions

HRT: performed experimental assays; SAM: provided scientific guidance for the project and reviewed the manuscript; GG: performed data analysis; MM: supervised the study plan; SS: supervised and conducted the study plan.

Data availability

All relevant data can be found within the manuscript.

Competing interests

The authors declare that they have no competing interests.

Funding

This research was partially funded by the Pasteur Institute of Iran (Tehran, Iran) for the fulfillment of Ph.D. thesis of Hasan Rahimi-Tamandegani (the first author).

Supplementary information

The online version contains supplementary material.

REFERENCES

1. Bray F, Laversanne M, Sung H, Ferlay J, Siegel RL, Soerjomataram I, et al. Global cancer statistics 2022: GLOBOCAN estimates of incidence and mortality worldwide for 36 cancers in 185 countries. *CA Cancer J Clin.* 2024;74(3):229-63.
2. Siegel RL, Wagle NS, Cercek A, Smith RA, Jemal A. Colorectal cancer statistics. 2023. *CA Cancer J Clin.* 2023;73(3):233-54.
3. Siegel RL, Kratzer TB, Giaquinto AN, Sung H, Jemal A. Cancer statistics, 2025. *CA Cancer J Clin.* 2025;75(1):10-45.
4. Toloudi M, Apostolou P, Papisotiriou I. Efficacy of 5-FU or oxaliplatin monotherapy over combination therapy in colorectal cancer. *J Cancer Ther.* 2015;6(4):345-55.
5. Miyazaki K, Shibahara T, Sato D, Uchida K, Suzuki H, Matsui H, et al. Influence of chemotherapeutic agents and cytokines on the expression of 5-fluorouracil-associated enzymes in human colon cancer cell lines. *J Gastroenterol.* 2006;41(2):140-50.
6. Villar-Grimalt A, Candel MT, Massuti B, Lizon J, Sanchez B, Frau A, et al. A randomized phase II trial of 5-fluorouracil, with or without human interferon- β , for advanced colorectal cancer. *Br J Cancer.* 1999;80(5-6):786-91.
7. Breul J, Jakse G, Forster G, Lampel A, Rohani A, Hartung R. 5-fluorouracil versus folinic acid and 5-fluorouracil in advanced, hormone-resistant prostate cancer: A prospective, randomized pilot trial. *Eur Urol.* 1997;32(3):280-3.
8. Fotheringham S, Mozolowski GA, Murray EM, Kerr DJ. Challenges and solutions in patient treatment strategies for stage II colon cancer. *Gastroenterol Rep.* 2019;7(3):151-61.
9. Qayum A, Magotra A, Shah SM, Nandi U, Sharma P, Shah BA, et al. Synergistic combination of PMBA and 5-fluorouracil (5-FU) in targeting mutant KRAS in 2D and 3D colorectal cancer cells. *Heliyon.* 2022;8(4):09103.
10. Taghizadeh H, Prager GW. Personalized adjuvant treatment of colon cancer. *Visc Med.* 2020;36(5):397-406.
11. Larsson I, Uhlén M, Zhang C, Mardinoglu A. Genome-scale metabolic modeling of glioblastoma reveals promising targets for drug development. *Front Genet.* 2020;11:381.
12. Robinson JL, Nielsen J. Anticancer drug discovery through genome-scale metabolic modeling. *Curr Opin Syst Biology.* 2017;4:1-8.
13. Zhang M, Saad C, Le L, Halfter K, Bauer B, Mansmann UR, et al. Computational modeling of methionine cycle-based metabolism and DNA methylation and the implications for anti-cancer drug response prediction. *Oncotarget.* 2018;9(32):22546-58.
14. Agren R, Mardinoglu A, Asplund A, Kampf C, Uhlen M, Nielsen J. Identification of anticancer drugs for hepatocellular carcinoma through personalized genome-scale metabolic modeling. *Mol Syst Biol.* 2014;10(3):721.
15. Turanli B, Zhang C, Kim W, Benfeitas R, Uhlen M, Arga KY, et al. Discovery of therapeutic agents for prostate cancer using genome-scale metabolic modeling and drug repositioning. *EBioMedicine.* 2019;42:386-96.
16. Murphy RA, Mourtzakis M, Chu QS, Baracos VE, Reiman T, Mazurak VC. Supplementation with fish oil increases first-line chemotherapy efficacy in patients with advanced nonsmall cell lung cancer. *Cancer.* 2011;117(16):3774-80.
17. Gao X, Sanderson SM, Dai Z, Reid MA, Cooper DE, Lu M, et al. Dietary methionine links nutrition and metabolism to the efficacy of cancer therapies. *Nature.* 2019;572(7769):397-401.
18. Paccagnella A, Morello M, Da Mosto MC, Baruffi C, Marcon ML, Gava A, et al. Early nutritional intervention improves treatment tolerance and outcomes in head and neck cancer patients undergoing concurrent chemoradiotherapy. *Support Care Cancer.* 2010;18(7):837-45.
19. Kuo Y-R, Lin C-H, Lin W-S, Pan M-H. L-Glutamine substantially improves 5-fluorouracil-induced intestinal mucositis by modulating gut microbiota and maintaining the integrity of the gut barrier in mice. *Mol Nutr Food Res.* 2024;68(9):2300704.
20. Chen Z, Xu J, Fang K, Jiang H, Leng Z, Wu H, et al. FOXO1-mediated serine metabolism reprogramming enhances colorectal cancer growth and 5-FU resistance under serine restriction. *Cell Commun Signal.* 2025;23(1):13.
21. Jornada DH, Boreski D, Chiba DE, Ligeiro D, Luz

- MAM, Gabriel EA, et al. Synergistic enhancement of 5-fluorouracil chemotherapeutic efficacy by taurine in colon cancer rat model. *Nutrients*. 2024;16(18):3047.
22. Gao X, Sanderson SM, Dai Z, Reid MA, Cooper DE, Lu M, et al. Dietary methionine influences therapy in mouse cancer models and alters human metabolism. *Nature*. 2019;572(7769):397-401.
 23. Colaprico A, Silva TC, Olsen C, Garofano L, Cava C, Garolini D, et al. TCGAAbiolinks: An R/Bioconductor package for integrative analysis of TCGA data. *Nucleic Acids Res*. 2016;44(8):71.
 24. Becker SA, Palsson BO. Context-specific metabolic networks are consistent with experiments. *Plos Comput Biol*. 2008;4(5):1000082.
 25. Agren R, Bordel S, Mardinoglu A, Pornputtapong N, Nookaew I, Nielsen J. Reconstruction of genome-scale active metabolic networks for 69 human cell types and 16 cancer types using INIT. *Plos Comput Biol*. 2012;8(5):1002518.
 26. Gustafsson J, Anton M, Roshanzamir F, Jörnsten R, Kerkhoven EJ, Robinson JL, et al. Generation and analysis of context-specific genome-scale metabolic models derived from single-cell RNA-Seq data. *Proc Natl Acad Sci U S A*. 2023;120(6):2217868120.
 27. Heirendt L, Arreckx S, Pfau T, Mendoza SN, Richelle A, Heinken A, et al. Creation and analysis of biochemical constraint-based models using the COBRA Toolbox v. 3.0. *Nat Protoc*. 2019;14(3):639-702.
 28. Agren R, Liu L, Shoaie S, Vongsangnak W, Nookaew I, Nielsen J. The RAVEN toolbox and its use for generating a genome-scale metabolic model for *Penicillium chrysogenum*. *Plos Comput Biol*. 2013;9(3):1002980.
 29. Fouladiha H, Marashi S-A, Torkashvand F, Mahboudi F, Lewis NE, Vaziri B. A metabolic network-based approach for developing feeding strategies for CHO cells to increase monoclonal antibody production. *Bioprocess Biosyst Eng*. 2020;43(8):1381-9.
 30. Chou T-C. Theoretical basis, experimental design, and computerized simulation of synergism and antagonism in drug combination studies. *Pharmacol Rev*. 2006;58(3):621-81.
 31. De Angelis PM, Svendsrud DH, Kravik KL, Stokke T. Cellular response to 5-fluorouracil (5-FU) in 5-FU-resistant colon cancer cell lines during treatment and recovery. *Mol Cancer*. 2006;5(1):20.
 32. Rodrigues D, de Souza T, Coyle L, Di Piazza M, Hershers B, Ferreira S, et al. New insights into the mechanisms underlying 5-fluorouracil-induced intestinal toxicity based on transcriptomic and metabolomic responses in human intestinal organoids. *Arch Toxicol*. 2021;95(8):2691-718.
 33. Sharma S, Zhang X, Azhar G, Patyal P, Verma A, Kc G, et al. Valine improves mitochondrial function and protects against oxidative stress. *Biosci Biotechnol Biochem*. 2024;88(2):168-76.
 34. Houten SM, Dodatko T, Dwyer W, Violante S, Chen H, Stauffer B, et al. Acyl-CoA dehydrogenase substrate promiscuity: Challenges and opportunities for development of substrate reduction therapy in disorders of valine and isoleucine metabolism. *J Inherit Metab Dis*. 2023;46(5):931-42.
 35. Taniguchi K, Nonami T, Nakao A, Harada A, Kurokawa T, Sugiyama S, et al. The valine catabolic pathway in human liver: Effect of cirrhosis on enzyme activities. *Hepatology*. 1996;24(6):1395-8.
 36. Guo Y, Wu J, Wang M, Wang X, Jian Y, Yang C, et al. The metabolite saccharopine impairs neuronal development by inhibiting the neurotrophic function of glucose-6-phosphate isomerase. *J Neurosci*. 2022;42(13):2631-46.
 37. Hallen A, Jamie JF, Cooper AJ. Lysine metabolism in mammalian brain: An update on the importance of recent discoveries. *Amino Acids*. 2013;45(6):1249-72.
 38. Guertin DA, Wellen KE. Acetyl-CoA metabolism in cancer. *Nat Rev Cancer*. 2023;23(3):156-72.
 39. Bidgood CL, Philp LK, Rockstroh A, Lehman M, Nelson CC, Sadowski MC, et al. Targeting valine catabolism to inhibit metabolic reprogramming in prostate cancer. *Cell Death Dis*. 2024;15(7):513.
 40. Yang J, Song C, Zhan X. The role of protein acetylation in carcinogenesis and targeted drug discovery. *Front Endocrinol*. 2022;13:972312.
 41. Takahara T, Amemiya Y, Sugiyama R, Maki M, Shibata H. Amino acid-dependent control of mTORC1 signaling: A variety of regulatory modes. *J Biomed Sci*. 2020;27(1):87.
 42. Park JM, Park HM, Kim WJ, Kim HU, Kim TY, Lee SY. Flux variability scanning based on enforced objective flux for identifying gene amplification targets. *BMC Systems Biology*. 2012;6(1):106.
 43. Liu J, Gao Q, Xu N, Liu L. Genome-scale reconstruction and in silico analysis of *Aspergillus terreus* metabolism. *Mol Biosyst*. 2013;9(7):1939-48.
 44. Jordan A, Stein J. Effect of an omega-3 fatty acid containing lipid emulsion alone and in combination with 5-fluorouracil (5-FU) on growth of the colon cancer cell line Caco-2. *Eur J Nutr*. 2003;42(6):324-31.